Journal of Molecular Catalysis A: Chemical 330 (2010) 99–106

Contents lists available at ScienceDirect

Journal of Molecular Catalysis A: Chemical

journal homepage: www.elsevier.com/locate/molcata

# DFT studies on the reaction mechanism of cross-metathesis of ethylene and 2-butylene to propylene over heterogeneous Mo/HBeta catalyst

Xin Li[a,b], Jing Guan[a], Anmin Zheng[c], Danhong Zhou[a,d], Xiuwen Han[a], Weiping Zhang[a,*], Xinhe Bao[a,*]

[a] State Key Laboratory of Catalysis, Dalian Institute of Chemical Physics, Chinese Academy of Sciences, 457 Zhongshan Road, Dalian 116023, China
[b] Graduate University of Chinese Academy of Sciences, Beijing 100049, China
[c] State Key Laboratory of Nuclear Magnetic Resonance and Atomic and Molecular Physics, Wuhan Institute of Physics and Mathematics, Chinese Academy of Sciences, Wuhan 430071, China
[d] Institute of Chemistry for Functionalized Material, College of Chemistry and Chemical Engineering, Liaoning Normal University, Dalian 116029, China

ARTICLE INFO

*Article history:*
Received 18 May 2010
Received in revised form 2 July 2010
Accepted 6 July 2010
Available online 13 July 2010

*Keywords:*
DFT calculations
Mo/HBeta catalyst
Olefin metathesis
Reaction mechanism
Active species

ABSTRACT

Density functional theory (DFT) calculations were performed to study the detailed reaction mechanism of the cross-metathesis of ethylene and 2-butylene over heterogeneous Mo/HBeta catalysts. The whole process is divided into two stages: the initiation of Mo–carbene species from Mo-oxo precursors and the propagating process by these active sites to yield propylene. The formation of initial Mo–carbene takes place via the endothermic addition and the subsequent decomposition of the oxametallacyclobutane intermediate. In the propagating stage to yield the final products, Mo=$CHCH_3$ firstly reacts with ethylene to form Mo=$CH_2$, which would further react with 2-butylene to give another propylene molecule. The oxidation states of the Mo species have great influences on the reactivities associated with these two stages. It is unfavorable for $Mo^{IV}$-oxo precursors to produce Mo–alkylidene species compared with $Mo^{VI}$ and $Mo^{V}$ sites. The energy barriers indicate that the $Mo^{VI}$ and $Mo^{V}$–alkylidene species could catalyze the olefin metathesis reaction, but $Mo^{V}$ ones are more preferred to be the active sites. The calculation results are consistent with our previous XPS results.

© 2010 Elsevier B.V. All rights reserved.

## 1. Introduction

Olefin metathesis has received considerable attention as it offers a powerful route for producing the desired chemical products through C–C bond formation. In recent years, the metathesis of ethylene and 2-butylene to produce propylene has attracted more and more interest due to the increasing demand of propylene in the word-wide market. Heterogeneous catalysts for this reaction are of particular interest due to the easier separation, good persistence, and recyclability. Various transition-metal compounds have been tested, the most feasible of which are those based on Re, Mo, W deposited on high surface-area supports such as $SiO_2$ and $Al_2O_3$ [1–5]. Recently, we reported that Mo/HBeta catalyst exhibits activity for the cross-metathesis of ethylene and 2-butylene to propylene, and higher reactivity would be obtained after addition of $Al_2O_3$ into the carrier [6,7]. Various characterizations have been used to detect the interfacial interaction between the Mo species and the support as well as their structures [8–10]. The oxidation states of the Mo species have important influences on the activities. Our XPS results indicated that deep reduction of Mo species to $Mo^{IV}$ may be responsible for the catalysts deactivation, and $Mo^{V}$ species are probably the active sites [11].

However, the reaction mechanism of olefin metathesis on heterogeneous catalyst has not been fully understood up to now. This could be due to too small amount of active sites to be detected with the current spectroscopic techniques [12]. The theoretical study is a good tool to investigate the catalyst structure and catalysis mechanism [13–17]. As far as the olefin metathesis is concerned, metal–carbene species are usually known as the initiation and propagating intermediates in both homogeneous and heterogeneous olefin metathesis [18–21]. While the mechanism to form the initial carbene is still not well known. Several mechanisms have been proposed in the past years [22–27]. It is reported that ethylidene can be obtained by dissociation of acetaldehyde on $\beta$-$Mo_2C$ [26]. Recently, Salameh et al. have found that the Re–carbene species can be created following the pseudo-Wittig mechanism on $Re_2O_7/Al_2O_3$ catalyst, which involves the formation and decomposition of a four-membered oxametallacyclobutane intermediate [27]. For the next propagating process catalyzed by the metal carbene, many theoretical studies are focused on Mo catalysts supported on $Al_2O_3$ or $SiO_2$ [28–31]. In calculations little attention has been paid when using zeolite as the support for olefin metathesis. In the present work, the two processes mentioned above have been studied to reveal the mechanism of cross-metathesis of ethy-

* Corresponding authors. Tel.: +86 411 8437 9976; fax: +86 411 8469 4447.
*E-mail addresses:* wpzhang@dicp.ac.cn (W. Zhang), xhbao@dicp.ac.cn (X. Bao).

1381-1169/$ – see front matter © 2010 Elsevier B.V. All rights reserved.
doi:10.1016/j.molcata.2010.07.007

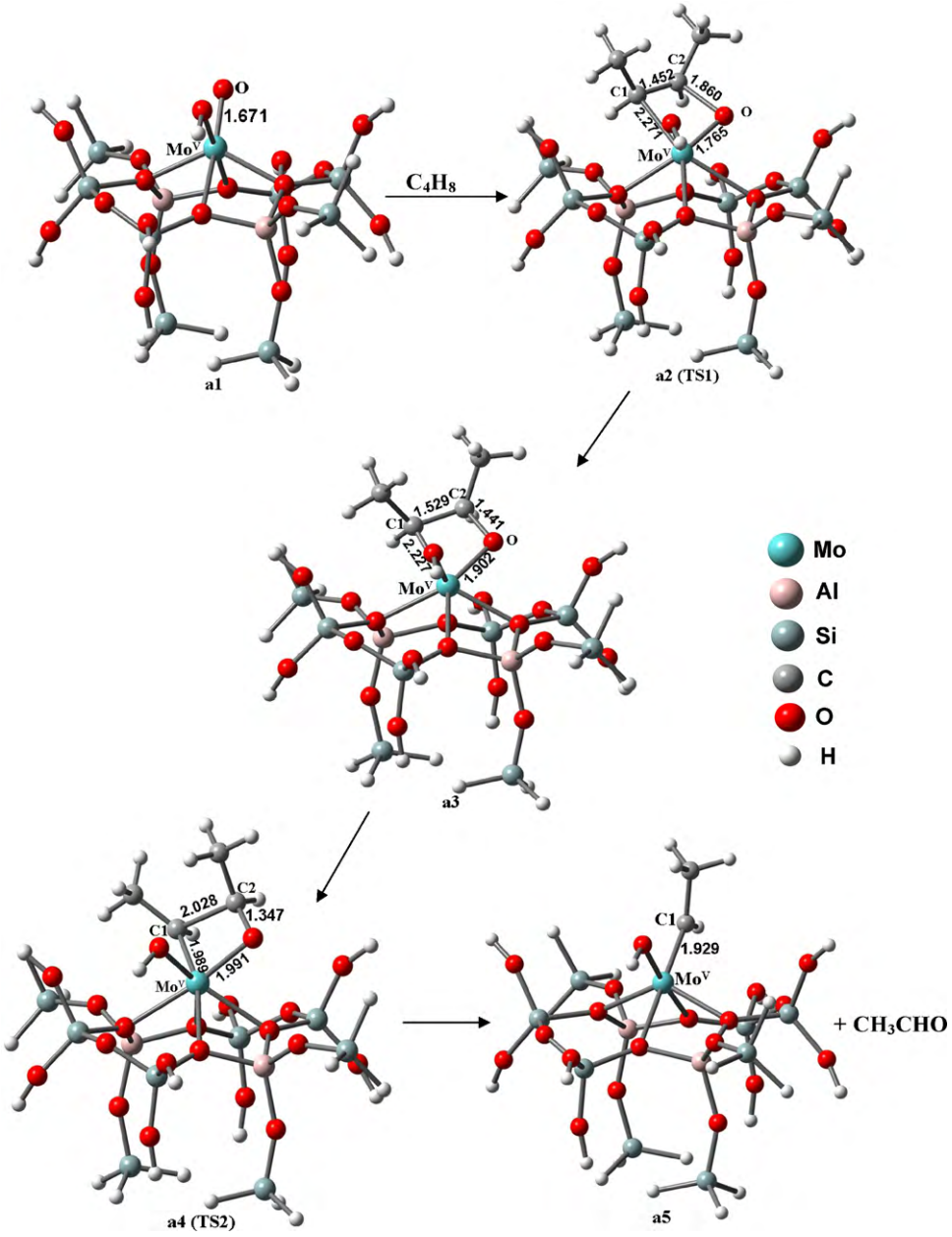


**Fig. 1.** The energy-minima (**a1**, **a3**, **a5**) and the transition states (**a2**, **a4**) along the pathway of $Mo^{V}$–ethylidene formation.

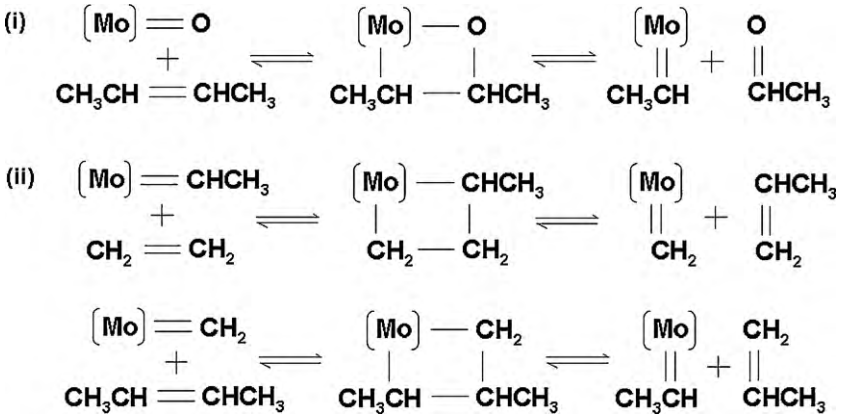


**Scheme 1.** The reaction pathways of ethylene and 2-butene cross-metathesis.

lene and 2-butene to propylene on Mo/HBeta zeolite catalyst using density functional theory. Meanwhile, the role of the Mo oxidation states in metathesis reaction is also investigated. Along with the reaction mechanism, the correlation between the oxidation states of the Mo species in Mo/HBeta catalyst and their olefin metathesis reactivity is also discussed.

## 2. Computational method

As reported in our previous work [32–34], a cluster approach was applied to model the active site for olefin metathesis reaction. The zeolite Beta model was taken from the framework structure of Polymorph A [35], which has a three-dimensional network of 12-membered rings. As suggested by the $^{27}$Al MQ MAS NMR results, the Al atoms were preferred to take place of the T1 or T2 sites [36]. Accordingly, we used the T1T1/6MR cluster models with two Al atoms located at two T1 sites in the six-membered ring to simulate the structure of HBeta zeolite. The proposed $Mo^{IV}O^{2+}$, $Mo^{V}O(OH)^{2+}$ and $Mo^{VI}O_2^{2+}$ precursors were assumed to be exchanged with a pair of Brönsted acid sites to anchor on the zeolite. The dangling bonds of the clusters model were terminated by H atoms, directing towards to the next lattice oxygen or silicon atom at a distance of 1.500 or 1.000 Å. In order to retain the local geometries of Beta zeolite, the boundary OH and $SiH_3$ groups were fixed in their crystallographic positions while other atoms were relaxed during the structure optimization.

All the calculations were performed using Gaussian03 software package [37]. The hybrid B3LYP functional was used, which combines the Becke's exchange and Lee et al. correlation function [38–41]. The LANL2DZ basis set including the Hay–Wadt [42] effective core potential (ECP) plus double-zeta basis was applied for Mo element and 6-31G (d, p) basis set applied for other non-transition elements (C, H, O, Al and Si). For the transition state structures of cross-metathesis reaction, the frequency calculations were carried out to check that the point exhibits only one negative frequency. All the energies reported have been corrected by zero point energies (ZPE), but no intramoleular BSSE correction was done.

## 3. Results and discussion

### 3.1. The initiation stage of Mo–ethylidene formation from Mo-oxo precursor

#### 3.1.1. $Mo^{V}$-oxo precursor

As depicted in Scheme 1(i), the production of Mo–alkylidene species follows the pseudo-Wittig mechanism via the formation and decomposition of an oxamolybdacyclobutane intermediate. On the basis of the activation barriers, our previous results have revealed that the formation of $Mo^{VI}$=$CHCH_3$ species is preferred compared to the $Mo^{VI}$=$CH_2$ species when 2-butylene and ethylene reacting with $Mo^{VI}$-oxo precursors [43]. In addition, the *syn*-$Mo^{VI}$=$CHCH_3$ species with the $CH_3$ group opposite to the zeolite framework was preferred over the *anti*-isomer. Thus in the following work, *syn*-Mo=$CHCH_3$ is considered as the dominant initial carbene species. Similar to our previous calculations on the $Mo^{VI}$-oxo precursors, $Mo^{V}$ and $Mo^{IV}$-oxo precursors were also chosen to explore the effect of the metal oxidation states on the initiation stage.

The cluster models of $Mo^{V}$-oxo precursor **a1** as well as the structures along the pathway of 2-butylene reacting with **a1** are presented in Fig. 1, with some selected geometrical parameters listed. An oxamolybdacyclobutane intermediate **a3** is characterized by the formation of two new bonds of Mo–$C_1$ and $C_2$–O with the length of 2.227 and 1.440 Å, respectively, accompanying by the obvious bonds length increase of Mo=O (from 1.671 Å in **a1** to 1.902 Å in intermediate **a3**) and $C_1$–$C_2$ (from 1.338 Å in isolated 2-butylene to 1.529 Å in **a3**). Then the oxamolybdacyclobutane species would be decomposed to produce **a5** and $CH_3CHO$. Two transition states **a2** (TS1) and **a4** (TS2) are found during the intermediate formation and decomposition processes. Both of them have nearly flat rings with the Mo–$C_1$–O–$C_2$ dihedral angle at 157.9 and −176.4°, respectively. The transition state **a2** is characterized by the activation of the butylene molecule and the formation of Mo–$C_1$ bond, which is only 0.044 Å longer than that in the oxamolybdacyclobutane intermediate **a3**. As the reaction proceeds, the $C_1$–$C_2$ bond is expected to be elongated further, and the $C_2$–O bond would be shortened. In transition state **a4**, the $C_1$–$C_2$ bond is elongated so much that the butylene molecule is decomposed, and the product $CH_3CHO$ is formed. Finally, the $Mo^{V}$–$CHCH_3$ (**a5**) active site with a Mo–$C_1$ distance of 1.929 Å is generated, which is the character of Mo=C double bond [28]. Furthermore, the Mulliken charge analysis shows that an electrophilic attack of $Mo^{V}$-oxo precursor to the π-bond of 2-butylene occurs in the **a3** formation at the level of 0.32 e.

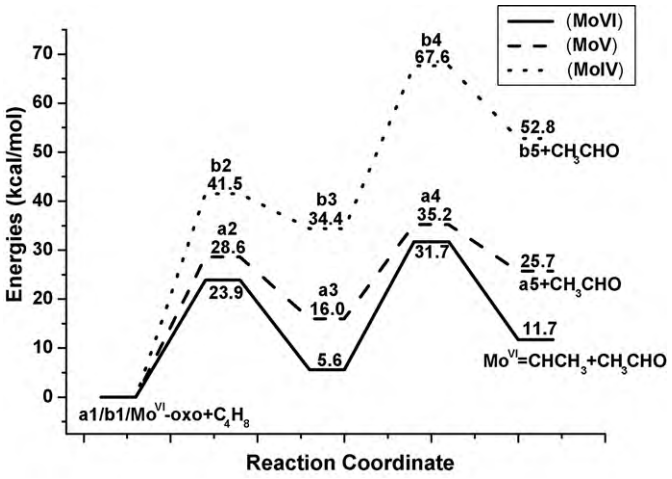


**Fig. 2.** The potential energy surfaces for the Mo–ethylidene formation starting from $Mo^{V}$ and $Mo^{IV}$ precursor (energy units in kcal/mol). The sum energies of **a1** + $C_4H_8$ or **b1** + $C_4H_8$ were set as the zero point in each path. The line of $Mo^{VI}$–ethylidene formation is from Ref. [43].

The energy diagram of 2-butylene reacting with $Mo^{V}$-oxo precursor **a1** to produce $Mo^{V}$=$CHCH_3$ **a5** is graphically presented in Fig. 2. It is shown that the formation of the intermediate **a3** is endothermic ($\Delta E$ = 16.0 kcal/mol) with an energy barrier of 28.6 kcal/mol when the sum energies of (**a1** + $C_4H_8$) are set as the zero points. While in the following step, it needs a much lower energy barrier of 19.2 kcal/mol to form $Mo^{V}$=$CHCH_3$ and $CH_3CHO$. The overall formation of the $Mo^{V}$=$CHCH_3$ active site is endothermic with a reaction heat of 25.7 kcal/mol. The energy calculated is slightly higher and can't be changed obviously by extending the used basis set [32]. This may be responsible for the induction period detected in the experiments [44,45]. For comparison, the energy diagram of 2-butylene reacting with $Mo^{VI}$-oxo precursor to produce $Mo^{VI}$=$CHCH_3$ species is also presented in Fig. 2. The sum energies of $Mo^{VI}$-oxo and $C_4H_8$ are set as the zero points in the pathway [43]. It is found that the $Mo^{VI}$ site is slightly efficient in producing the initial Mo=$CHCH_3$ species compared to the $Mo^{V}$ one.

#### 3.1.2. $Mo^{IV}$-oxo precursor

The structures of the species along the pathway of $Mo^{IV}$=$CHCH_3$ formation with $Mo^{IV}$-oxo precursor **b1** are given in Fig. 3. Unlike the $Mo^{V}$-oxo precursor, the $Mo^{IV}$ one has only one oxo-O ligand, the same to that $Mo^{IV}$ supported on silica [46]. A [2 + 2] cycloaddition reaction of Mo=O and $C_1$=$C_2$ bonds occurs to form an intermediate

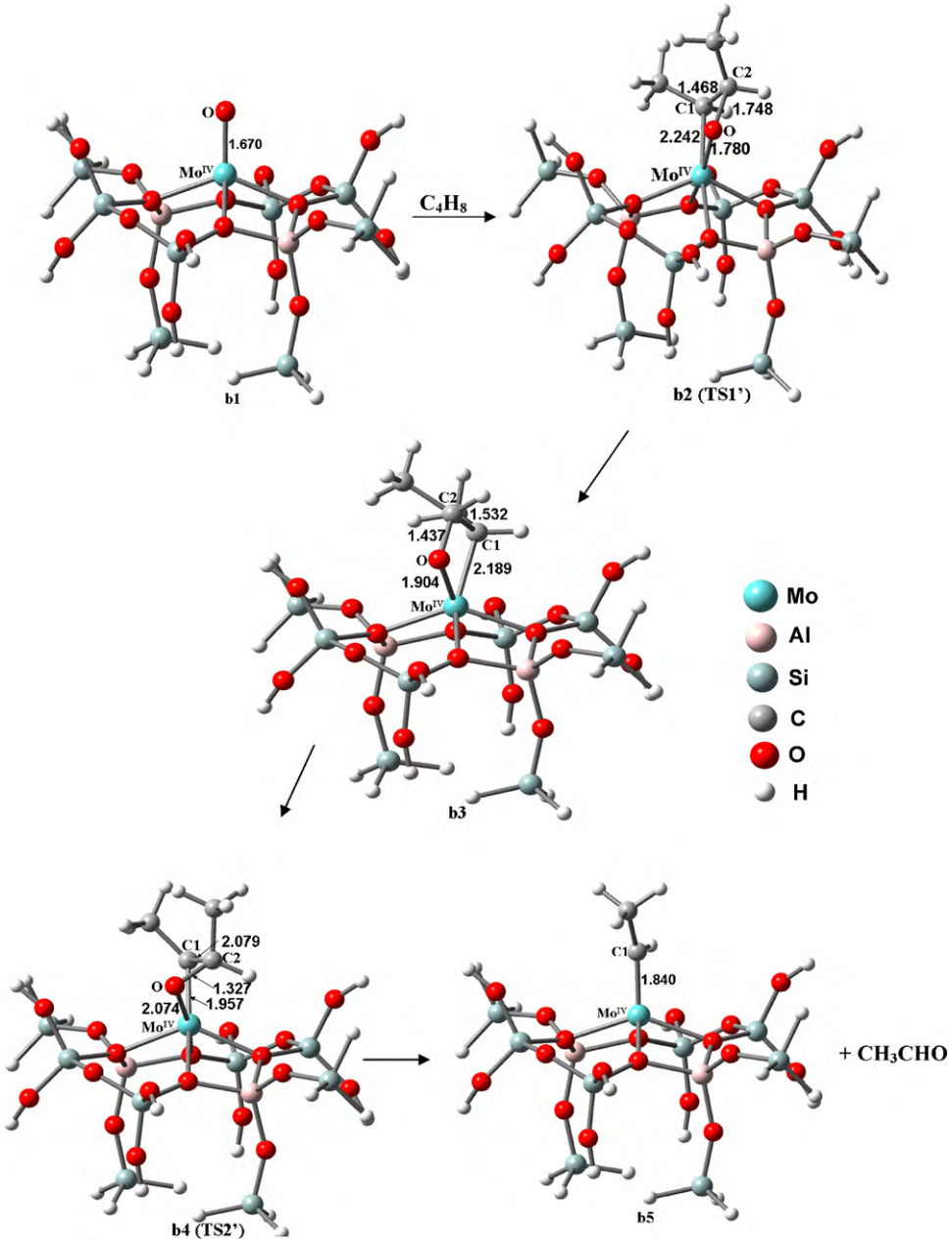


**Fig. 3.** The energy-minima (**b1**, **b3**, **b5**) and the transition states (**b2**, **b4**) along the pathway of $Mo^{IV}$–ethylidene formation.

**b3** when 2-butylene reacts with $Mo^{IV}$-oxo precursor. Comparing the energy-minima and transition state geometries, it is found that the reaction pathways over $Mo^{V}$ and $Mo^{IV}$-oxo precursors have many geometrical similarities except that the lengths of formed $Mo^{IV}$–C bond are shorter than the corresponding $Mo^{V}$ ones. Furthermore, lower electronic charge transfer (0.23 e) from 2-butylene to $Mo^{IV}$-oxo precursor is observed, which can be attributed to the less electrophilic property of the $Mo^{IV}$ center (1.20 e in **b1**).

The energy profile of generating $Mo^{IV}$=$CHCH_3$ **b5** active site is also presented in Fig. 2 with the sum energies of **b1** and $C_4H_8$ setting as zero point. It is endothermic to form the intermediate **b3** from $Mo^{IV}$-oxo precursor ($\Delta E$ = 34.4 kcal/mol) with an activation barrier of 41.5 kcal/mol. However, the decomposition of the intermediate to $Mo^{IV}$=$CHCH_3$ and $CH_3CHO$ occurs with a lower energy barrier (33.2 kcal/mol). The overall reaction heat is estimated to be 52.8 kcal/mol. Comparing the energy changes in each path, it is found that the initiation reaction occurred on $Mo^{IV}$-oxo precursor **b1** has the highest activation barrier (kinetics) and reaction energy (thermodynamics) than that on the $Mo^{VI}$ and $Mo^{V}$-oxo species. So, $Mo^{IV}$-oxo precursor is not favorable for producing the initial carbene according to pseudo-Wittig mechanism. Accordingly, the $Mo^{IV}$–carbene is excluded in the following calculations. Similarly, it is reported that the active centers of ethylene metathesis do not contain $Mo^{IV}$–carbene on $Mo/Al_2O_3$ catalyst [28].

### 3.2. The propagating stage of Mo–alkylidene to produce propylene

As mentioned above, the Mo=$CHCH_3$ sites are supposed to be the dominant initial species on the catalyst surface. The propagating stage of Mo–carbene to the final product is shown in the Scheme 1(ii): Mo=$CHCH_3$ first reacts with ethylene to form Mo=$CH_2$ and propylene, then the Mo=$CH_2$ would react with 2-butylene to produce another Mo=$CHCH_3$ and propylene to finish

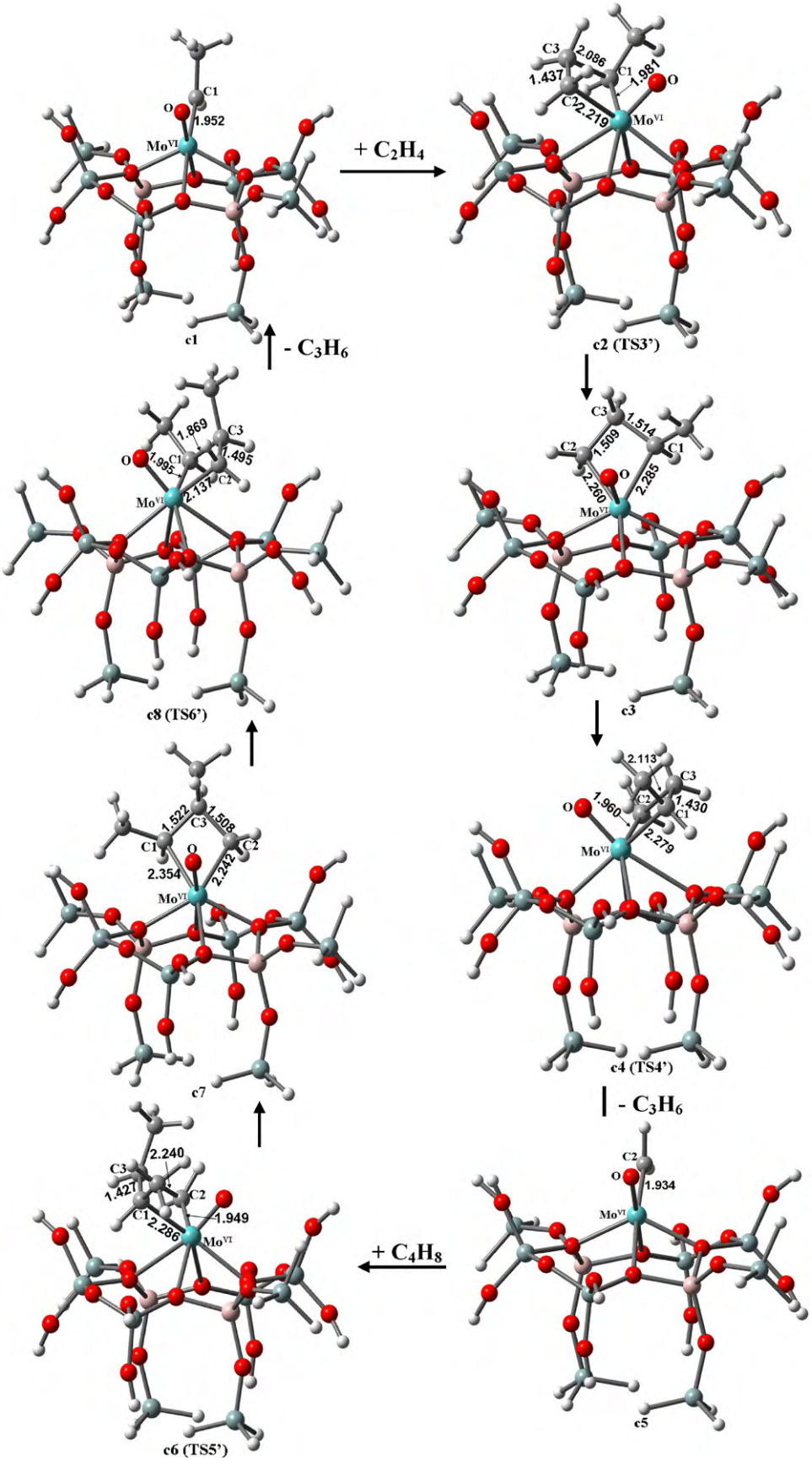


**Fig. 4.** The energy-minima (**c1**, **c3**, **c5**, **c7**) and the transition states (**c2**, **c4**, **c6**, **c8**) along the pathway of $Mo^{VI}$–alkylidene species reacting with alkene to produce propylene.

the catalytic cycle. The degenerate metathesis reactions are not considered here.

### 3.2.1. $Mo^{VI}$–alkylidene active site

The energy-minimum and transition state structures in the propagating process of $Mo^{VI}$–carbene active sites reacting with alkenes are presented in Fig. 4. Two types of carbene species of $Mo^{VI}$=$CHCH_3$ (**c1**) and $Mo^{VI}$=$CH_2$ (**c5**) are involved. Some selected geometrical parameters are also presented. First, ethylene can attack $Mo^{VI}$=$CHCH_3$ **c1** to form a molybdacyclobutane intermediate **c3** with a methyl substituent connected to $C_1$ atom. It has a four-member ring with the Mo–$C_1$–$C_2$–$C_3$ dihedral angle of 159.2. The bond lengths of Mo–$C_1$ and Mo–$C_2$ in **c3** are 2.285 and 2.260 Å, respectively, which are characteristic of the Mo–C single bond. It can be seen that the structure of **c3** is much like to a puckered metallacycle other than a flat one, which is different to that reported in the literature [28] and may be due to the different catalyst system and different Mo environment. In order to produce propylene, the intermediate **c3** has to be decomposed to form $Mo^{VI}$=$CH_2$ **c5** and propylene. Two transition states **c2** (TS3′) and **c4** (TS4′) are located corresponding to the four-membered ring's closing and opening. In the formation of transition state **c2**, $C_2$=$C_3$ bond in ethylene is activated and Mo–$C_2$ bond is significantly formed ahead of the $C_1$–$C_3$ bond. This is also consisted with the previous reports [28]. Accordingly, in the transition state **c4**, the $C_2$–$C_3$ bond is almost cleaved to form propylene, and another metal–carbene active site $Mo^{VI}$=$CH_2$ **c5** is produced.

The next step is accomplished by the addition of 2-butylene to $Mo^{VI}$=$CH_2$ **c5** to yield the starting $Mo^{VI}$=$CHCH_3$ **c1** active site and another propylene molecule. Two transition states **c6** (TS5′) and **c8** (TS6′) are localized, connected by the molybdacyclobutane intermediate **c7**. Similar changes to that mentioned in the first step bas been observed between the structures of energy-minimum and transition state species. Mulliken charge analysis shows that there is little electron transfer from alkenes to Mo–carbenes (0.1–0.2 e) in the whole process.

Energy diagrams of the propagating process of $Mo^{VI}$=$CHCH_3$ active site to produce propylene are presented in Fig. 5. It is found that the reaction of ethylene and $Mo^{VI}$=$CHCH_3$ **c1** is preferred with a slightly lower activation barrier than the next step with $Mo^{VI}$=$CH_2$. In first step, the formation of the molybdacyclobutane intermediate **c3** is a little endothermic ($\Delta E$ = 0.3 kcal/mol) with an activation barrier of 12.7 kcal/mol, whereas its decomposition needs 13.0 kcal/mol to take place. The overall reaction heat associated with this process is estimated to be 3.9 kcal/mol. In the second step of 2-butylene addition to $Mo^{VI}$=$CH_2$ **c5**, it has to overcome a higher activation barrier of 15.2 kcal/mol to form the molybdacyclobutane intermediate **c7**, which would be cleaved to produce the initial $Mo^{VI}$=$CHCH_3$ **c1** species with an activation barrier of 8.8 kcal/mol. The overall reaction is exothermic with the $\Delta E$ of −5.5 kcal/mol.

### 3.2.2. $Mo^{V}$–alkylidene active site

The structures associated with the propagating process of $Mo^{V}$=$CHCH_3$ with alkenes to produce propylene are presented in Fig. 6. It can be seen that the Mo oxidation state doesn't have significant effect on the Mo species conformations as the structure features of the $Mo^{V}$ series are similar to the $Mo^{VI}$ ones shown in Fig. 4. However, large discrepancies can be observed in the reaction activation barriers which showed in Fig. 5. In the first step catalyzed by $Mo^{V}$=$CHCH_3$ species, the formation of $Mo^{V}$-molybdacyclobutane intermediate **a7** is slightly exothermic ($\Delta E$ = −0.5 kcal/mol), suggesting that the reaction of $Mo^{V}$=$CHCH_3$ **a5** with ethylene is thermodynamically preferable. The activation energy for **a7** formation is at the level of 5.6 kcal/mol, which is only half of the value predicted for the $Mo^{VI}$=$CHCH_3$ (12.7 kcal/mol)

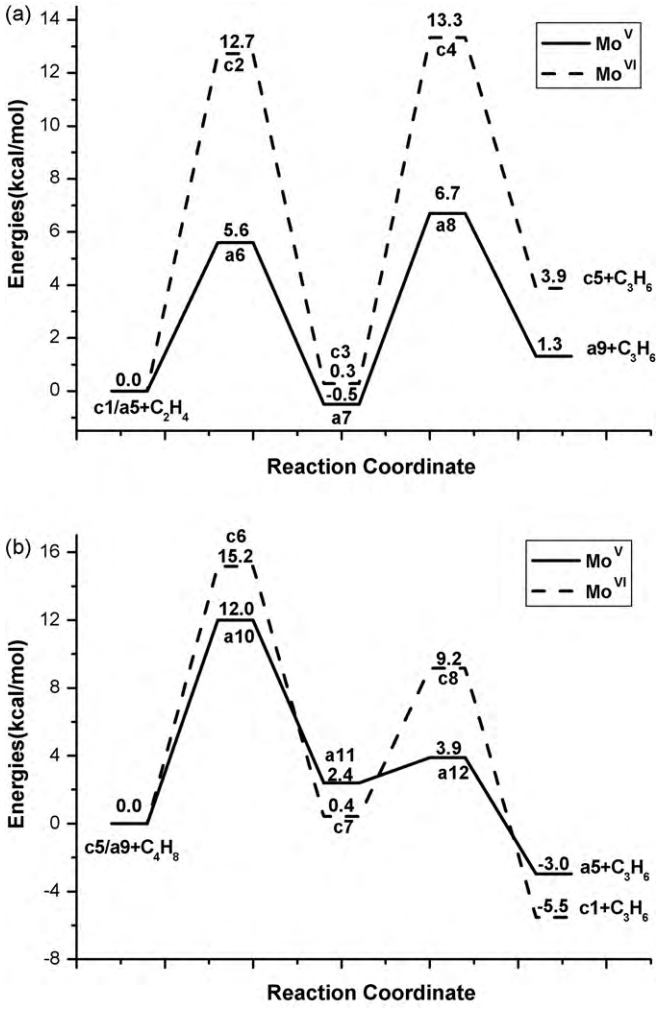


**Fig. 5.** The potential energy surfaces for the cross-metathesis reaction over $Mo^{VI}$ and $Mo^{V}$ carbene species (energy units in kcal/mol). In each case, the energies of **c1** + $C_4H_8$ or **a5** + $C_4H_8$ in (a) and **c5** + $C_2H_4$ or **a9** + $C_2H_4$ in (b) were set as the benchmarks, respectively.

active site. Meanwhile, the activation barrier of the intermediate **a7** conversion to $Mo^{V}$=$CH_2$ **a9** and propylene is also 5.8 kcal/mol lower than the corresponding $Mo^{VI}$ process. Thus, it is assumed that the $Mo^{V}$=$CHCH_3$ are more likely to react with ethylene compared to the $Mo^{VI}$ species. Moreover, it should be noted that the activation barrier (5.6 kcal/mol) of ethylene addition to $Mo^{V}$–ethylidene is lower than that previously found for ethylene addition to $Mo^{V}$–methylidene (14.2 kcal/mol) [33]. That means that ethylene is more likely to react with Mo=$CHCH_3$ than Mo=$CH_2$, similar to that happened on $Mo/Al_2O_3$ catalyst [29].

Subsequent reaction of the addition of 2-butylene to $Mo^{V}$=$CH_2$ **a9** is showed in Fig. 5(b). The formation of $Mo^{V}$ four-membered ring intermediate **a11** is endothermic ($\Delta$E = 2.4 kcal/mol) with the predicted activation barrier of 12.0 kcal/mol, which is smaller than that over $Mo^{VI}$=$CH_2$ **c5** site. In addition, the conversion of **a11** to the final product of $Mo^{V}$=$CHCH_3$ **a5** and propylene is more feasible than the decomposition of intermediate **c7** with almost zero activation barrier (1.5 kcal/mol). The reaction heat related with this step is exothermic ($\Delta E$ = −3.0 kcal/mol). Combining the above two steps, it can be seen that the first step of $Mo^{V}$=$CHCH_3$ reacting with $C_2H_4$ is more preferred to take place than the next step of $Mo^{V}$=$CH_2$ reacting with $C_4H_8$.

By comparing the activation barriers and reaction energies of the whole propagating processes over $Mo^{VI}$ and $Mo^{V}$–alkylidene

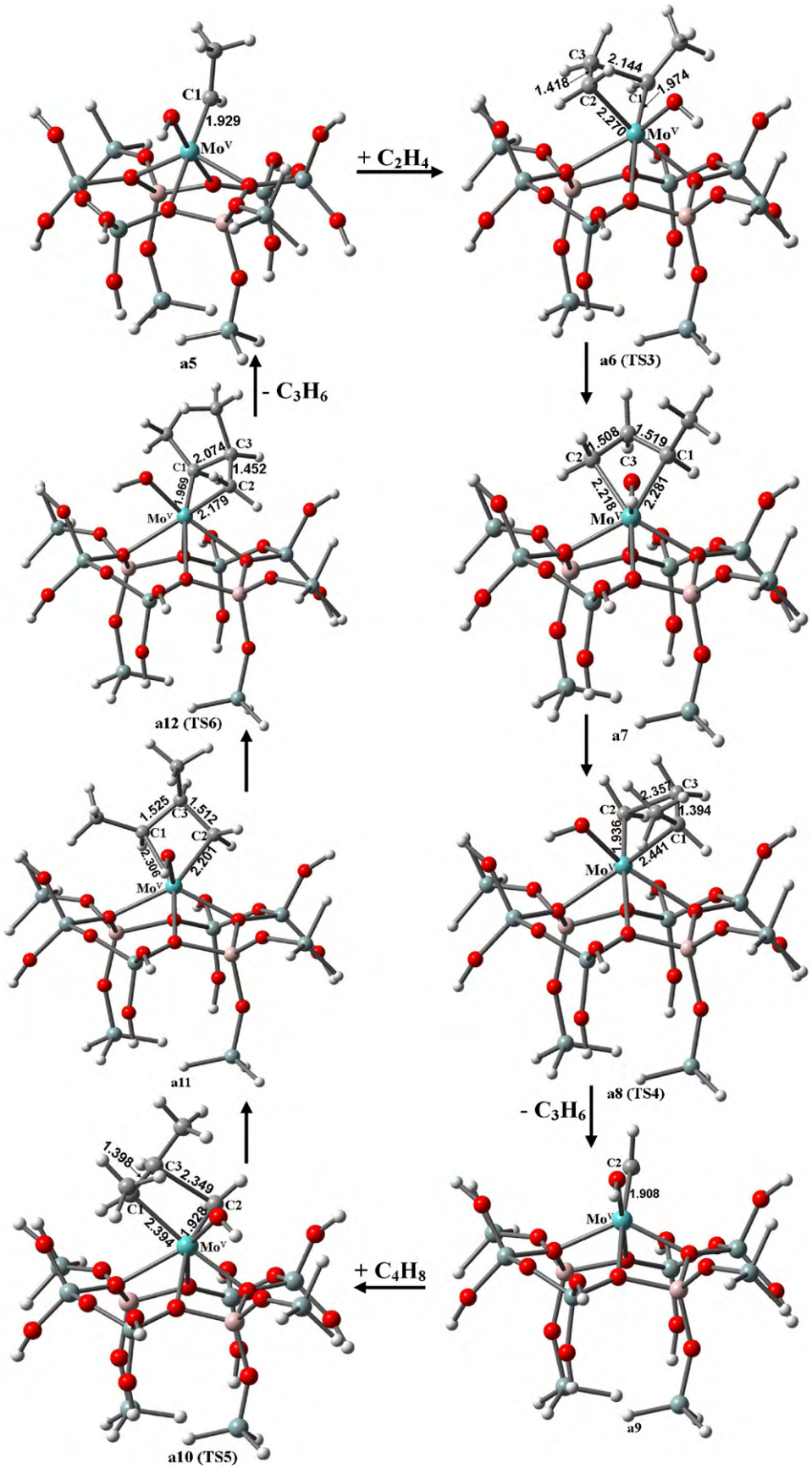


**Fig. 6.** The energy-minima (**a5**, **a7**, **a9**, **a11**) and the transition states (**a6**, **a8**, **a10**, **a12**) along the pathway of ethylene and 2-butylene cross-metathesis over $Mo^{V}$–alkylidene.

active sites, it indicates that the $Mo^{V}$–alkylidene species is more preferable than the $Mo^{VI}$ one to catalyze the olefin metathesis in terms of the reaction kinetics and thermodynamics. Therefore, our theoretical results have shown that the $Mo^{V}$–alkylidene species are probably the active sites in this cross-metathesis reaction over Mo/HBeta catalyst.

As discussed above, two steps occur on the heterogeneous Mo/HBeta catalyst in the production of propylene from the cross-metathesis between ethylene and 2-butylene: the initiation of Mo–carbenes from Mo-oxo precursors and the propagating of these active sites with alkenes. From the energy analysis, it seems that the oxidation state of Mo center in metal–carbene active site would have great influences on the catalytic performance in the metathesis reaction. The deep reduced $Mo^{IV}$ species would be excluded from the active sites for their high energy barriers. As the propagation process catalyzed by Mo–carbene is the main reaction compared to the first initial carbene formation step, it assumes that the $Mo^{V}$ one would be preferred to be the active site compared to the $Mo^{VI}$ species. Our previous experimental XPS spectra of fresh, deactivated and regenerated Mo based catalysts in the cross-metathesis of ethylene and 2-butylene to propylene showed that deep reduction of Mo species to $Mo^{IV}$ is the reason of the catalyst deactivation [11]. So avoiding the deep reduction of the catalyst is important for its further application in industry. Meanwhile our XPS results demonstrate that $Mo^{V}$ species are formed gradually during the reaction, which are probably the active sites [11]. The theoretical calculations in this study also support our previous experimental conclusions.

## 4. Conclusions

The detailed reaction mechanism of the cross-metathesis of ethylene and 2-butylene to produce propylene over heterogeneous Mo/HBeta catalyst were investigated by DFT calculations. The whole process contains two stages: the initiation of Mo–carbene species from Mo-oxo precursors and the propagating of these active sites with ethylene and 2-butylene to yield propylene. It is found that the Mo–carbene is produced via two elementary reaction steps i.e., the endothermic formation and subsequent opening of the four-membered rings of the oxametallacyclobutane intermediates. The $Mo{=}CHCH_3$ species are taken as the dominant initial carbenes on the surface of the catalysts. In the propagating reaction of Mo–carbenes to the final products, two kinds of metal carbenes were considered. First, $Mo{=}CHCH_3$ reacts with ethylene to produce $Mo{=}CH_2$, which would further reacts with 2-butylene to give propylene.

The reactivities of the Mo active sites are dependent on their oxidation states. In the initiation stage, the activation barriers and overall reaction heats are estimated to be significantly higher on $Mo^{IV}$ sites compared with $Mo^{VI}$ and $Mo^{V}$-oxo precursors, indicating that the $Mo^{IV}$-oxo precursors are hardly to be formed the initial $Mo^{IV}{=}CHCH_3$ active site according to pseudo-Wittig mechanism. In the propagating stage, both the energy barriers and reaction heats are found to be lower in the case of $Mo^{V}$–alkylidene rather than in the $Mo^{VI}$. As the propagating stage is the main process taking place in the experiment, it is assumed that the $Mo^{V}$–alkylidene species are probably the active sites.

## Acknowledgments

We gratefully acknowledge the financial support of the National Natural Science Foundation of China (Grant nos. 20403017 and 20873140) and the Ministry of Science and Technology of China through the National Key Project of Fundamental Research (Grant no. 2009CB623507).

## References

[1] J.C. Mol, Catal. Today 51 (1999) 289.
[2] R. Spronk, J.A.R. van Veen, J.C. Mol, J. Catal. 144 (1994) 72.
[3] J.C. Mol, J. Mol. Catal. A 213 (2004) 39.
[4] B. Mitra, X.T. Gao, I.E. Wachs, A.M. Hirt, G. Deo, Phys. Chem. Chem. Phys. 3 (2001) 1144.
[5] Y. Inaki, H. Yoshida, K. Kimura, S. Inagaki, Y. Fukushima, T. Hattori, Phys. Chem. Chem. Phys. 2 (2000) 5293.
[6] S.L. Liu, S.J. Huang, W.J. Xin, J. Bai, S.J. Xie, L.Y. Xu, Catal. Today 93–95 (2004) 471.
[7] X.J. Li, W.P. Zhang, S.L. Liu, L.Y. Xu, X.W. Han, X.H. Bao, J. Catal. 250 (2007) 55.
[8] X.J. Li, W.P. Zhang, S.L. Liu, X.W. Han, L.Y. Xu, X.H. Bao, J. Mol. Catal. A 250 (2006) 94.
[9] X.J. Li, W.P. Zhang, S.L. Liu, L.Y. Xu, X.W. Han, X.H. Bao, J. Phys. Chem. C 112 (2008) 5955.
[10] X. Li, W.P. Zhang, X.J. Li, S.L. Liu, Prog. Chem. 20 (2008) 1021.
[11] X.J. Li, W.P. Zhang, X. Li, S.L. Liu, H.J. Huang, X.W. Han, L.Y. Xu, X.H. Bao, J. Phys. Chem. C 113 (2009) 8228.
[12] J. Handzlik, J. Ogonowski, Catal. Lett. 88 (2003) 119.
[13] M. Boronat, P. Concepción, A. Corma, M.T. Navarro, M. Renz, S. Valencia, Phys. Chem. Chem. Phys. 11 (2009) 2876.
[14] S.F. Vyboishchikov, M. Bühl, W. Thiel, Chem. Eur. J. 8 (2002) 3962.
[15] Y.D. Wu, Z.H. Peng, J. Am. Chem. Soc. 119 (1997) 8043.
[16] L. Cavallo, J. Am. Chem. Soc. 124 (2002) 8965.
[17] G. Sastre, Phys. Chem. Chem. Phys. 9 (2007) 1052.
[18] R.H. Grubbs, Tetrahedron 60 (2004) 7117.
[19] R.R. Schrock, J. Mol. Catal. A 213 (2004) 21.
[20] C. Adlhart, P. Chen, J. Am. Chem. Soc. 126 (2004) 3496.
[21] J. Handzlik, P. Sautet, J. Catal. 256 (2008) 1.
[22] D.T. Laverty, J.J. Rooney, A. Stewart, J. Catal. 45 (1976) 110.
[23] F.M. Alias, M.L. Poveda, M. Sellin, E. Carmona, J. Am. Chem. Soc. 120 (1998) 5816.
[24] G. Wu, W.T. Tysoe, Surf. Sci. 397 (1998) 197.
[25] X. Chen, X. Zhang, P. Chen, Angew. Chem. Int. Ed. 42 (2003) 3798.
[26] M. Siaj, C. Reed, S.T. Oyama, S.L. Scott, P.H. McBreen, J. Am. Chem. Soc. 126 (2004) 9514.
[27] A. Salameh, C. Coperet, J.M. Basset, V.P.W. Bohm, M. Roper, Adv. Synth. Catal. 349 (2007) 238.
[28] J. Handzlik, J. Ogonowski, J. Mol. Catal. A 175 (2001) 215.
[29] J. Handzlik, J. Catal. 220 (2003) 23.
[30] J. Handzlik, J. Phys. Chem. B 109 (2005) 20794.
[31] J. Handzlik, J. Mol. Catal. A 316 (2010) 106.
[32] J. Guan, G. Yang, D.H. Zhou, W.P. Zhang, X.C. Liu, X.W. Han, X.H. Bao, J. Mol. Catal. A 300 (2009) 41.
[33] X. Li, J. Guan, D.H. Zhou, G.H. Li, X.W. Han, W.P. Zhang, X.H. Bao, J. Mol. Struct. Theo. 913 (2009) 167.
[34] X. Li, A.M. Zheng, J. Guan, X.W. Han, W.P. Zhang, X.H. Bao, Catal. Lett. 138 (2010) 116.
[35] J.M. Newsam, M.M.J. Treacy, W.T. Koetsier, C.B. De Gruyter, Proc. R. Soc. Lond. A 420 (1988) 375.
[36] J.A. van Bokhoven, D.C. Koningsberger, P. Kunkeler, H. van Bekkum, A.P.M. Kentgens, J. Am. Chem. Soc. 122 (2000) 12842.
[37] M.J. Frisch, G.W. Trucks, H.B. Schlegel, G.E. Scuseria, M.A. Robb, J.R. Cheeseman, J.A. Montgomery Jr., T. Vreven, K.N. Kudin, J.C. Burant, J.M. Millam, S.S. Iyengar, J. Tomasi, V. Barone, B. Mennucci, M. Cossi, G. Scalmani, N. Rega, G.A. Petersson, H. Nakatsuji, M. Hada, M. Ehara, K. Toyota, R. Fukuda, J. Hasegawa, M. Ishida, T. Nakajima, Y. Honda, O. Kitao, H. Nakai, M. Klene, X. Li, J.E. Knox, H.P. Hratchian, J.B. Cross, C. Adamo, J. Jaramillo, R. Gomperts, R.E. Stratmann, O. Yazyev, A.J. Austin, R. Cammi, C. Pomelli, J.W. Ochterski, P.Y. Ayala, K. Morokuma, G.A. Voth, P. Salvador, J.J. Dannenberg, V.G. Zakrzewski, S. Dapprich, A.D. Daniels, M.C. Strain, O. Farkas, D.K. Malick, A.D. Rabuck, K. Raghavachari, J.B. Foresman, J.V. Ortiz, Q. Cui, A.G. Baboul, S. Clifford, J. Cioslowski, B.B. Stefanov, G. Liu, A. Liashenko, P. Piskorz, I. Komaromi, R.L. Martin, D.J. Fox, T. Keith, M.A. Al-Laham, C.Y. Peng, A. Nanayakkara, M. Challacombe, P.M.W. Gill, B. Johnson, W. Chen, M.W. Wong, C. Gonzalez, J.A. Pople, Gaussian 03, Revision B. 05, Gaussian, Inc., Pittsburgh PA, 2003.
[38] A.D. Becke, Phys. Rev. A 38 (1988) 3098.
[39] A.D. Becke, J. Chem. Phys. 98 (1993) 5648.
[40] B. Miehlich, A. Savin, H. Stoll, H. Preuss, Chem. Phys. Lett. 157 (1989) 200.
[41] C. Lee, W. Yang, G. Parr, Phys. Rev. B 37 (1988) 785.
[42] P.J. Hay, W.R. Wadt, J. Chem. Phys. 82 (1985) 299.
[43] J. Guan, G. Yang, D.H. Zhou, W.P. Zhang, X.C. Liu, X.W. Han, X.H. Bao, Catal. Commun. 9 (2008) 2213.
[44] M.J. Lewis, G.B. Wills, J. Catal. 15 (1969) 140.
[45] R.C. Luckner, G.E. Mcconchie, G.B. Wills, J. Catal. 28 (1973) 63.
[46] S. Chempath, Y.H. Zhang, A.T. Bell, J. Phys. Chem. C 111 (2007) 1291.